JNC TY9400 2005-019

Study on Pb-Bi Corrosion of Structural and Fuel Cladding Materials for Nuclear Applications (2)

Part II. Exposure of Weld P122 in Oxygen Containing Flowing LBE at 550 °C for 5,000h

August 2005

Japan Nuclear Cycle Development Institute
Forschungszentrum Karlsruhe GmbH

〒319-1184　茨城県那珂郡東海村村松 4 番地49

核燃料サイクル開発機構

技術展開部　技術協力課

電話:029-282-1122

ファックス:029-282-7980

電子メール:jserv@jnc.go.jp

Technical Cooperation Section,

Technology Management Division,

Japan Nuclear Cycle Development Institute

4-49 Muramatsu, Tokai-mura, Naka-gun, Ibaraki 319-1184, Japan

Study on Pb-Bi Corrosion of Structural and Fuel Cladding Materials for Nuclear Applications (2)

Part II. Exposure of Weld P122 in Oxygen Containing Flowing LBE at 550 °C for 5,000h

C. Schroer[*], Z. Voß[*], O. Wedemeyer[*], J. Novotny[*],
J. Konys[*], A. Heinzel[**], A. Weisenburger[**], G. Müller[**],
T. Furukawa[***], K. Aoto[***]

Abstract

This report summarises the results of exposure experiments on the behaviour of 12Cr-2W steel P122 joined by multi-run TIG welding in oxygen-containing flowing lead-bismuth eutectic (LBE) at 550°C for nominally 800, 2000 and 5000 h. The flow velocity of the LBE and the mean oxygen content were 2 m/s and 5×10-7 mass-% (aPbO = 10-3), respectively. The influence of surface-alloying with aluminium (GESA-treatment) was also investigated in an exposure experiment for nominally 5000 h.

The behaviour of the welded joint is generally comparable to that of P122 (after the standard heat-treatment), both qualitatively and quantitatively. Only few exceptions were observed which probably result from local peculiarities of the specific sample material. After surface alloying with aluminium, no significant oxidation and no liquid metal corrosion occurred in the centre of the specimens (including the weld seam), where the desired high quality of the aluminised layer was achieved.

[*] Institute for Materials Research III, Forschungszentrum Karlsruhe GmbH (FZK)

[**] Institute for Pulsed Power and Microwave Technology, FZK

[***] Advanced Material Research Group, Advanced Technology Division, O-arai Engineering Center, Japan Nuclear Cycle Development Institute

原子炉構造材料及び燃料材料の鉛ビスマス中腐食に関する研究(2)
第 2 報 P122 溶接継手の 550°C 酸素濃度制御流動鉛ビスマス中における 5000h 浸漬試験結果

C. Schroer[*], Z. Voß[*], O. Wedemeyer[*], J. Novotny[*],
J. Konys[*], A. Heinzel[**], A. Weisenburger[**], G. Müller[**],
古川智弘[***], 青砥紀身[***]

要　旨

本報告書は、P122（12Cr-2W）鋼 TIG 溶接継手の 550°C 酸素濃度制御流動鉛ビスマス（LBE）中における 800h、2,000h および 5,000h の腐食試験結果についてまとめたものである。LBE 流速および溶存酸素濃度は、それぞれ 2 m/s 、5×10^{-7} mass-% ($a_{PbO} = 10^{-3}$)である。鋼材の腐食に及ぼすアルミニウムによる表面改質（GESA 処理）効果についても評価を実施した。

溶接継手の腐食挙動は、定性的にも定量的にも熱処理が行われた母材のそれと同等であった。ごく一部に母材のそれとは異なる結果が得られたが、供試材の問題であると考えられた。溶接部の GESA 処理部分には、高温酸化、液体金属腐食ともに観察されず、良好な耐食性が観察された。

[*] 独国・カールスルーエ研究所、Institute for Materials Research III

[**] 独国・カールスルーエ研究所、Institute for Pulsed Power and Microwave Technology

[***] 核燃料サイクル開発機構　大洗工学センター　要素技術開発部　新材料研究グループ

Table of Contents

1 Introduction

The objective of this part of the "Study on Pb/Bi Corrosion of Structural and Fuel Cladding Materials for Nuclear Application" was to investigate the behaviour of a welded joint of 12Cr-2W steel P122 in oxygen-containing flowing lead-bismuth (LBE) at 550°C. Furthermore, the effect of surface-alloying of the weld with aluminium (GESA treatment) was examined. For this purpose, exposure experiments for up to 5000 h were performed in the CORRIDA loop at the Karlsruhe Lead Laboratory (KALLA) as part of the collaboration between the Japan Nuclear Cycle Development Institute (JNC) and the Karlsruhe Research Centre.

2 Sample Material

The welded plate of P122 (supplied by JNC) had a thickness of 30 mm and was joined by multi-run tungsten inert gas (TIG) welding. A schematic illustration of the structure of the joint which consists of 55-56 layers is shown in Figure 1. The chemical composition of the employed welding filler was very similar to that of the joined steel (Table 1), so that significant deviations in the average composition along the weld seam are not expected.

2.1 Machining of specimens

The part of the welded sample which contains the joint was separated from the plate by two cuts running parallel to the welding direction at a distance of approximately 20 mm from the centre of the weld seam. From the part which contains the joint, cylinders with dimensions Ø8×35 mm were cut with the long axis aligned perpendicular to the welding direction. The ends of these cylinders were provided with an internal and external (screw) thread according to the workshop drawing shown in Figure 2. The surface of the specimens was finished by turning.

The specimens for the exposure experiments were taken from two heats. Heat 1 was cut out of the top part of the weld where the single-V joint is comparatively broad and consists of two and more overlapping welding layers. Heat 2 was cut out of the middle part of the weld (Figure 1).

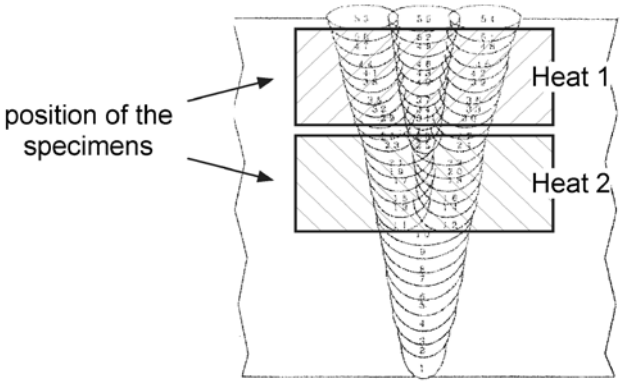

Figure 1 – *Schematic illustration of the structure of the joint (multi-run single-V butt joint) and position of the specimens for the exposure experiments.*

Table 1 – *Chemical composition (in mass-%) of the welded steel (P 122) and the filler material.*

P 122 (HCM12A, SUS410J3)										
Fe	Cr	W	Cu	Mn	Mo	Ni	Si	V	Nb	Al
bal. (84.69)	10.54	1.72	1.00	0.64	0.34	0.33	0.27	0.19	0.048	0.001
	C	N	B	P	S					
	0.11	0.071	0.034	0.016	0.002					
welding filler										
Fe	Cr	W	Cu	Mn	Mo	Ni	Si	V	Nb	Al
bal. (84.05)	10.5	1.43	1.51	0.52	0.26	1.04	0.3	0.2	0.05	n.a.
	C	N	B	P	S					
	0.09	0.0424	n.a.	0.005	0.002					
post-welding heat treatment of the welded plate (thickness: 30 mm): 1.5 h at 740°C (air cooling)										

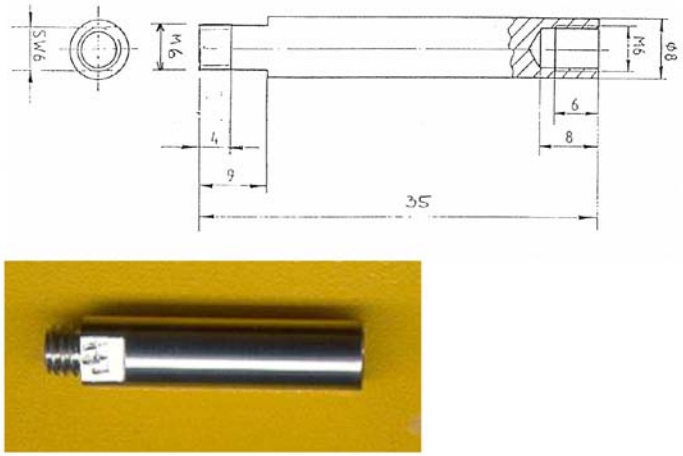

Figure 2 – *Workshop drawing according to which the specimens for the exposure experiments were machined and photograph of a finished specimen.*

Two specimens which were taken from Heat 1 were surface-alloyed with aluminium on one quarter of the specimen circumference in the GESA facility.

2.2 Basic characterisation of the specimens

Figure 3 gives an overview of the microstructure of the welded steel along the long axis of the cylindrical specimens (Heat 1). Three principal domains can be distinguished: (1) the welded steel (P122 after the post-welding heat-treatment); (2) an approximately 1¼ mm thick transition zone; and (3) the weld seam. Figure 3 also indicates the decreasing thickness of the V-joint from the top to the root of the weld. The section of the weld seam which is contained in specimens from Heat 2 is of more uniform thickness, similar to the bottom part of the section of the joint shown in Figure 3.

Figure 4 shows the microstructure of the joint in comparison to the microstructure of P122 after the post-welding heat-treatment (1.5 h at 740°C and subsequent air cooling). The weld seam consists of comparatively coarse grains which are stretched in the direction of the root of the weld. These coarse grains alternate with fine-grained domains (Figure 4 left). Macroscopic defects within the joint like pores and (comparatively big) slag inclusions which, if present in significant amounts, should become visible after polishing were not observed. This, of course, does not exclude the presence of microscopic inhomogeneities (e.g., sporadic, small inclusions; segregation) demanding more laborious metallographic methods of identification as those applied in this investigation (light-microscopic examination after polishing and etching).

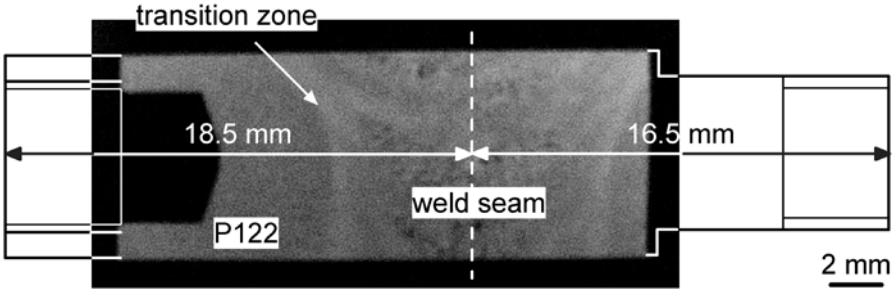

Figure 3 – *Cross-section along the long axis of a specimen taken from Heat 1 after etching with Röchling's solution (400 ml ethyl alcohol, 50 ml hydrochloric acid, 50 ml nitric acid, 6 g picric acid).*

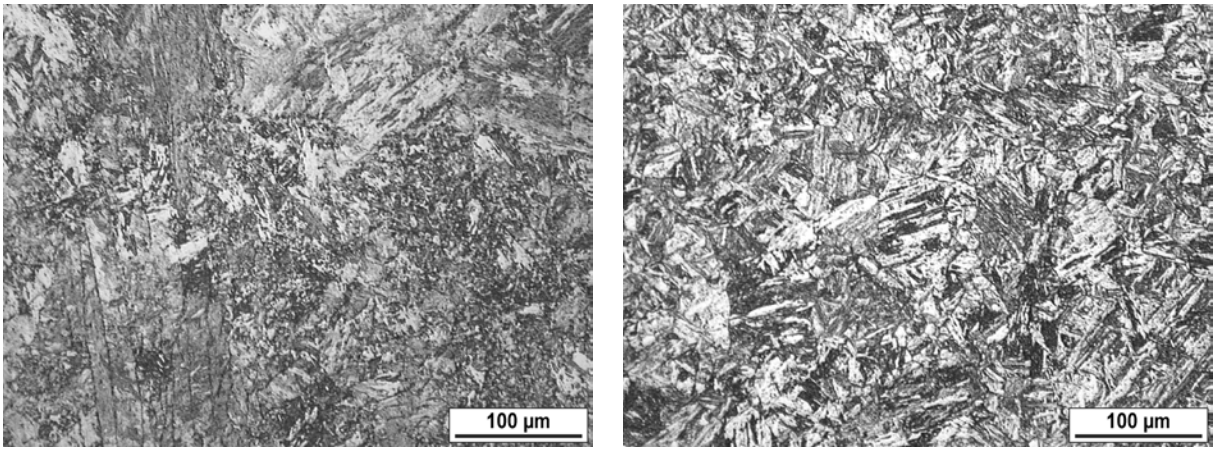

Figure 4 – *Microstructure of the weld seam (left) and P122 after the post-welding heat treatment (right). Etching: Röchling's solution.*

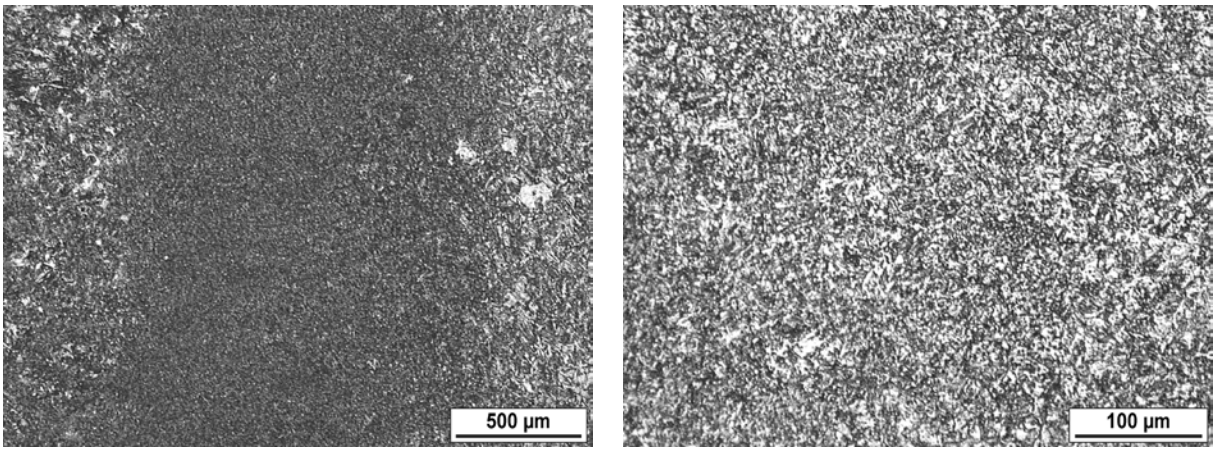

Figure 5 – *Microstructure of the transition zone between the weld seam (on the left in the left micrograph) and P 122 (on the right in the left micrograph). Etching: Röchling's solution.*

The transition zone which separates the weld seam from the welded steel is exceptionally fine-grained (Figure 5). This fine-grained domain may originate from rapid cooling at the edges of the molten weld pool due to fast dissipation of heat in the adjacent solid metal. In an analogous manner, the fine-grained domains within the weld seam may have formed where the single weld layers overlap.

3 Experimental

The exposure of specimens from the welded plate in oxygen-containing flowing lead-bismuth eutectic (LBE) at 550°C was performed in the CORRIDA loop (Figure 6), which provides two test-sections, each housing up to 18 of the cylindrical specimens. The specimens of the different steels tested simultaneously are connected to each other via the screw threads (*cf.* Figure 2). Within one circulation, the LBE first flows through Test-section 1 and subsequently passes Test-section 2.

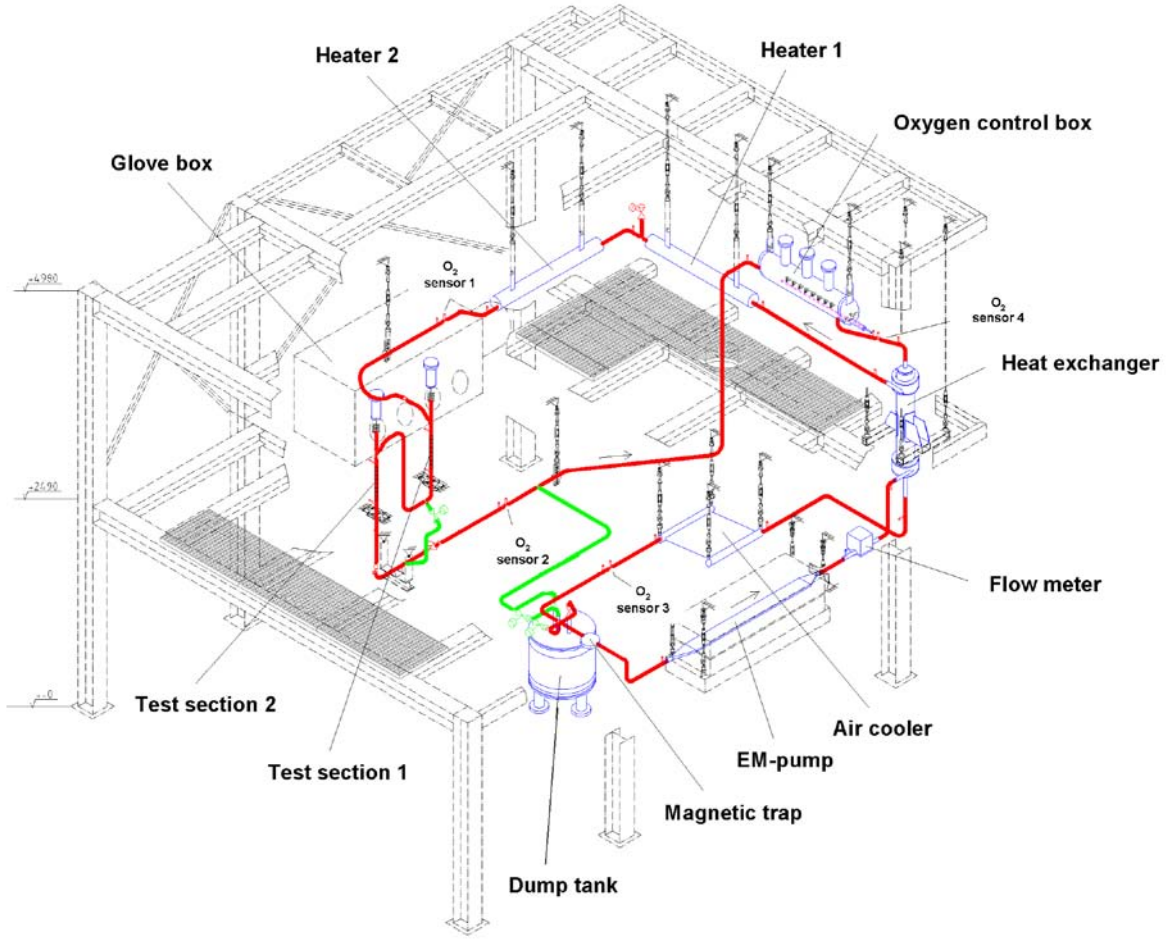

Figure 6 – *Schematic illustration of the CORRIDA loop (blue: components; red: flow path; green: additional tubing for emptying the loop). The oxygen activity in the circulating liquid metal is adjusted in the so-called "oxygen control box" via mass transfer between the liquid metal and a carrier gas (argon) with variable oxygen partial pressure at 550°C. The oxygen activity achieved in the liquid metal is recorded via oxygen sensors residing in selected positions along the loop. The maximum temperature along the loop is 550°C (test-sections, oxygen control box) and the minimum temperature is 380°C (inlet of the electromagnetic pump).*

3.1 Exposed specimens

The welded steel without GESA-treatment was exposed in the loop for nominally 800, 2000 and 5000 h. Four specimens were employed for each exposure time. Two of these four specimens resided in Test-section 1 and the other two in corresponding positions in Test-section 2, in order to investigate differences in the corrosive load between the test-sections. Specimens with a partly aluminised surface were exposed for nominally 5000 h only. In this case, only one specimen per test-section was used. The exact exposure times are given in Table 2, together with additional information on the employed specimens, including the heat they were taken from.

Before the experiments, the specimens were cleaned with acetone in an ultrasonic bath.

Table 2 – *List of the exposed specimens.*

specimen	heat	GESA-treatment	test section	exposure time (h)
S01	1	no	1	816
S02				
S03			2	
S04				
S05	1	no	1	2016
S06				
S07			2	
S08				
S09	2	no	1	4990
S10				
S11			2	
S12				
T02	1	yes	1	4990
T03			2	

3.2 Exposure conditions

An important parameter of the corrosion test is the oxygen content of the LBE which was controlled in the course of the experiments via oxygen transfer between the LBE and an argon-based carrier gas with adjustable oxygen partial pressure. The target of the oxygen control was 10^{-6} mass-%. The achieved oxygen content was measured using zirconia solid-electrolyte sensors residing in four selected positions along the loop (Figure 6). The most reliable signal was obtained from a sensor with Pt/air reference which resides near the inlet of Test-section 1 at 553°C.

The electromotive force (EMF) which was measured with this Pt/air sensor is shown in Figure 7. The EMF indicated by the sensor can be converted into the activity of lead oxide, a_{PbO}, which – with the assumption that Henry's law is valid – is (approximately) proportional to the mass concentration of oxygen, c_O, in the LBE. The factor of proportionality is the reciprocal value of the concentration in oxygen-saturated LBE, $c_{O;s}$, at the regarded temperature, i.e.,

$$\frac{c_O}{c_{O;s}} \approx \frac{x_O}{x_{O;s}} = \frac{x_{PbO}}{x_{PbO;s}} = a_{PbO} \qquad (1)$$

(x_i: molar concentration of substance i). For consistency with the other parts of this study, the saturation concentration of oxygen in LBE is calculated using the equation derived by Müller et al. [1],

$$\log\left(c_{O;s}/(\text{mass-\%})\right) = 2.52 - \frac{4803}{T/(K)} \qquad (2)$$

A more detailed discussion of the estimation of oxygen concentrations from the EMF indicated by oxygen sensors is given in the final report on the oxidation behaviour of P122 and a 9Cr-2W ODS-steel in flowing LBE.

The exposure conditions, which, with respect to the oxygen concentration, follow from Figure 7, are summarised in Table 3.

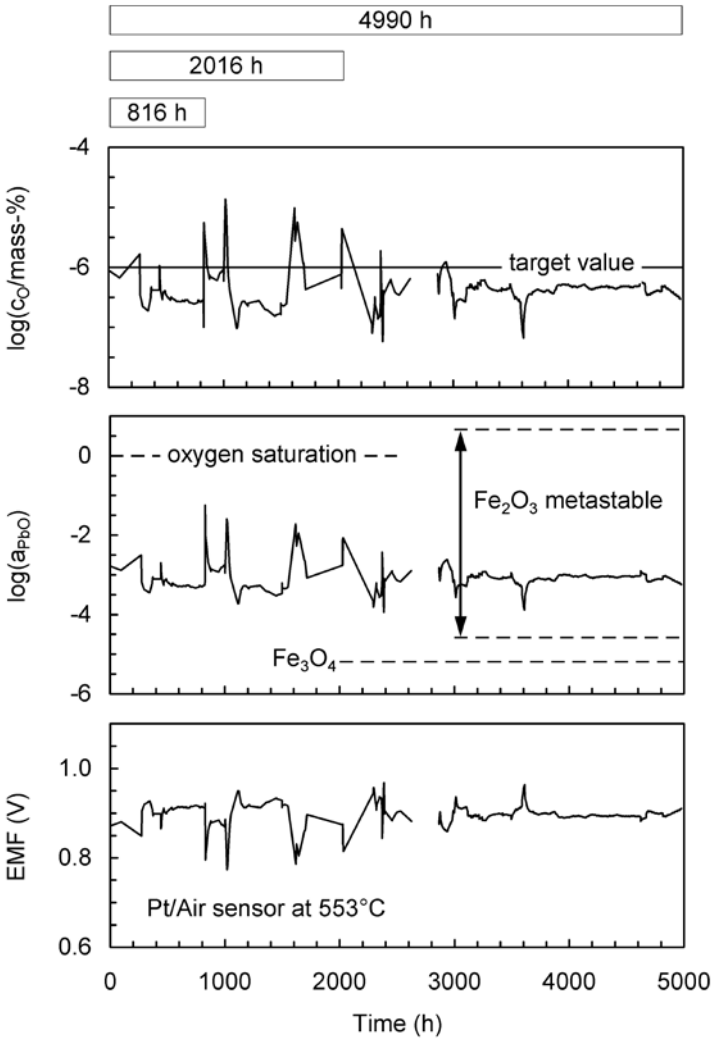

Figure 7 – *Record of the electromotive force (EMF) measured with the Pt/air sensor near the inlet of the first test-section as a function of time. The EMF was converted into the activity of lead oxide, a_{PbO}, and mass concentration of oxygen, c_O, using the saturation concentration of oxygen following from Equation (2). The bars at the top of the figure correspond to the exposure times in Table 2.*

Table 3 – *Summary of the testing conditions. Mean oxygen concentration and lead oxide activity according to Figure 7.*

composition of LBE						temperature (°C)	flow velocity (m/s)
Pb (mass-%)	Bi (mass-%)	O (mass-%)	a_{Pb}	a_{Bi}	a_{PbO}		
46	54	~5×10^{-7}	0.370	0.462	~10^{-3}	550	2.0 ± 0.2

3.3 Post-test examinations

Two of the four specimens from the welded plate which were exposed for the same time – one from each test-section – were retained for post-test examination at JNC. The remaining two were prepared for light- and electron-microscopy (supplemented

by energy-dispersive X-ray micro-analyses (EDX)). From one of these two specimens, both a longitudinal cross-section (along the long cylinder axis) exhibiting the welded steel, the transition zone and parts of the weld seam, and a vertical cross-section through the centre of the weld seam were produced (as illustrated in Figure 8). The second specimen was only investigated in longitudinal cross-section for comparison of the test-sections of the loop.

From the two specimens surface-alloyed with aluminium which were exposed for 5000 h (one in each test-section), one was retained for examination at JNC and the other was investigated in longitudinal cross-section.

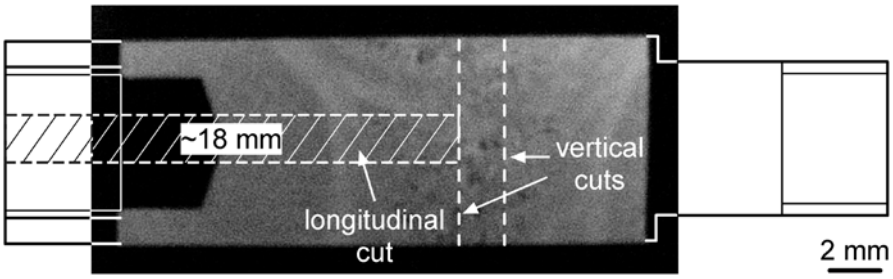

Figure 8 – *Illustration of the fragmentation of specimens of welded P122 for the post-test examinations.*

4 Oxidation Behaviour of P122

First, findings on the oxidation behaviour of P122 without weld after standard heat-treatment (massive block of ~200 mm thickness: 1.7 h at 1070°C (air cooling) + 7.3 h at 770°C) in flowing LBE at 550°C will briefly be summarised. These findings resulted from another part of the study on Pb/Bi corrosion and are described and discussed in-depth in the respective final report of the 1st research agreement between JNC and FZK.

After exposure to oxygen-containing flowing LBE at 550°C, P122 exhibits a non-uniform oxide scale which, in some domains, is comparatively thin (e.g., <1 µm after 2000 h) and most likely consists of a Cr-rich oxide of type α-Me_2O_3. Other parts of the surface are covered with a thicker oxide scale (~15 µm after 2000 h) which is composed of a (Fe,Cr) spinel layer and an internal oxidation zone. The formation of the thicker scale starts locally, where the thin Cr-rich scale did not form or lost its protective properties (Figure 9). These observations were made on specimens which – due to initial problems with the control of the oxygen content in the LBE – were exposed to LBE with varying oxygen content (c_O between 5×10^{-9} and 5×10^{-6} mass-%).

Information on the oxidation behaviour of P122 at permanently higher oxygen content in the LBE is available from a specimen which was exposed at $c_O \approx 5\times10^{-7}$ mass-% for 4990 h, simultaneously with the specimens from the welded plate. The structure of the oxide scale also significantly varies along the surface, but, in this case, domains with a continuous spinel layer alternate with sites where the spinel layer is in-

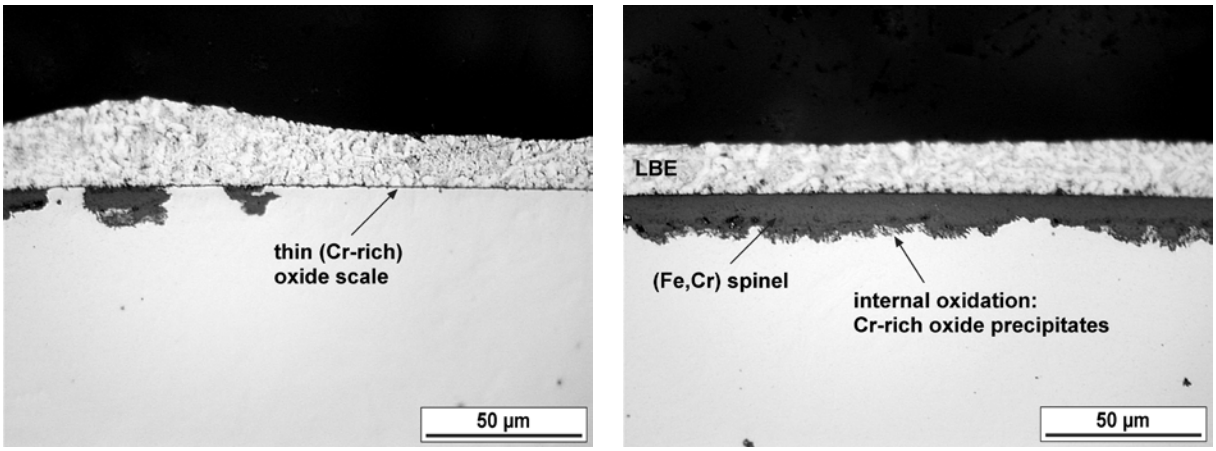

Figure 9 – *Oxide scale on the surface of P122 after exposure for 2018 h to flowing LBE at 550°C. The oxygen concentration in the LBE varied between 5×10^{-9} and 5×10^{-6} mass-%. Left: domain with a thin, protective scale and local spinel formation. Right: continuous spinel layer and internal oxidation along grain boundaries of the steel.*

terrupted by regions consisting of Cr-depleted steel, which resulted from non-uniform inward-growth of the spinel (Figure 10). Around such peaks in the instantaneous steel surface, parts of the spinel layer can be missing, most likely due to spalling during the exposure. An internal oxidation zone is mostly present beneath the spinel layer and at the surface of the Cr-depleted peaks in the steel surface which, after partial spalling of the spinel, also exceed the surface of the adherent part of the spinel layer. According to the current state of knowledge, partial spalling of the spinel around peaks in the steel surface is a long-term effect of the permanently high oxygen content in the flowing LBE.

Figure 11 summarises results of measurements of the oxide scale thickness for P122 after exposure to flowing LBE. The sum of the thickness of the spinel layer and the internal oxidation zone was thereby equated with the metal recession (loss of cross-

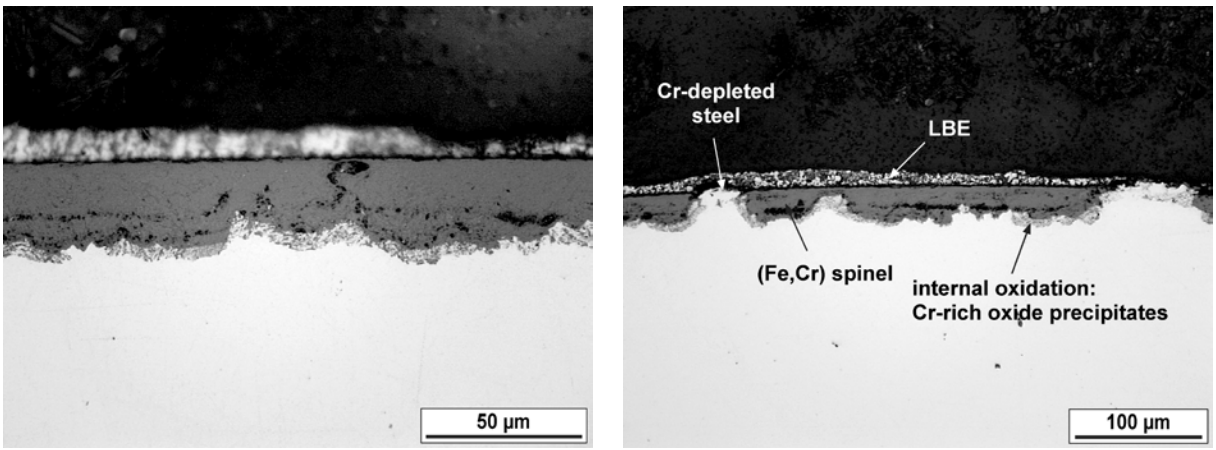

Figure 10 – *Cross-section of P122 after exposure for 4990 h to flowing LBE at 550°C and $c_O \approx 5\times10^{-7}$ mass-%. Left: continuous spinel layer and internal oxidation. Right: Cr-depleted peaks in the instantaneous steel surface interrupting the spinel layer.*

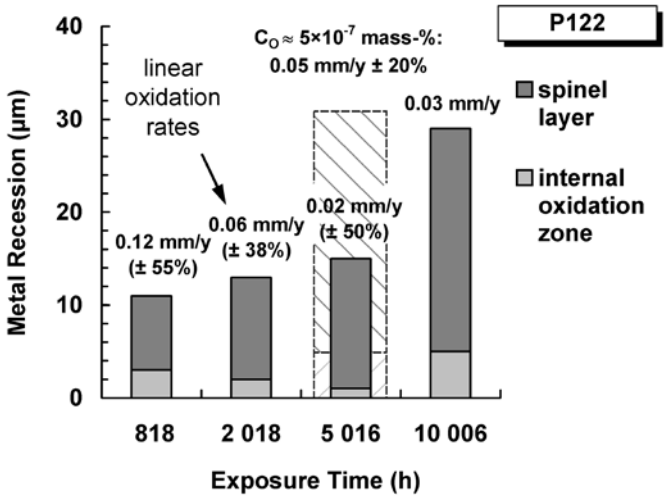

Figure 11 – *Metal recession (and resulting linear oxidation rates) of P122 after exposure to oxygen-containing flowing LBE at 550°C as estimated from the observed thicknesses of the spinel layer and the internal oxidation zone (mean values of twelve measurements each in a light-optical microscope at 500× magnification). Solid columns: the respective specimens were exposed to varying conditions with respect to the oxygen content (c_O between 5×10^{-10} and 5×10^{-6} mass-%). Hatched column: after exposure for 4990 h at $c_O \approx 5\times10^{-7}$ mass-%. The value for 5016 h was obtained from the reverse (non-aluminised) side of a GESA-treated specimen (ground instead of turned surface).*

section), since the surface of the (inward-growing) spinel layer normally coincides with the initial position of the steel surface [2]. The mean linear oxidation rates which follow from the metal recession are also shown in Figure 11.

Although the oxygen concentration periodically reached values as low as 5×10^{-10} mass-% ($a_{PbO} = 10^{-6}$) during some of these experiments, a direct reaction of the LBE with P122 (liquid metal corrosion) was never observed. Obviously, there was always an oxide scale on the surface which inhibited this deleterious type of corrosion. All these experiments, however, started with comparatively high oxygen concentrations (5×10^{-6} mass-% or $a_{PbO} = 10^{-2}$).

The presence of (outward-growing) Fe-oxide, i.e., magnetite, on top of the oxide scale is rarely observed in the case of oxidation of P122 in flowing LBE at 550°C. Especially the specimen which was exposed at comparatively high oxygen concentration (~5×10^{-7} mass-%) showed no Fe-oxide at all, although, from a thermodynamic point of view, magnetite formation was favoured in the course of the whole exposure period (5000 h). Also, after comparatively short exposure (818 h) at oxygen concentrations above the threshold for magnetite stability, no Fe-oxide was found.

5 Results and Discussion

5.1 Weld seam

Figure 12 shows different types of oxide scales which were found along the circumference of the weld seam (near the centre of the joint) after exposure at 550°C and $c_O \approx 5\times10^{-7}$ mass-% for 816 h. The weld seam predominantly exhibits the scale struc-

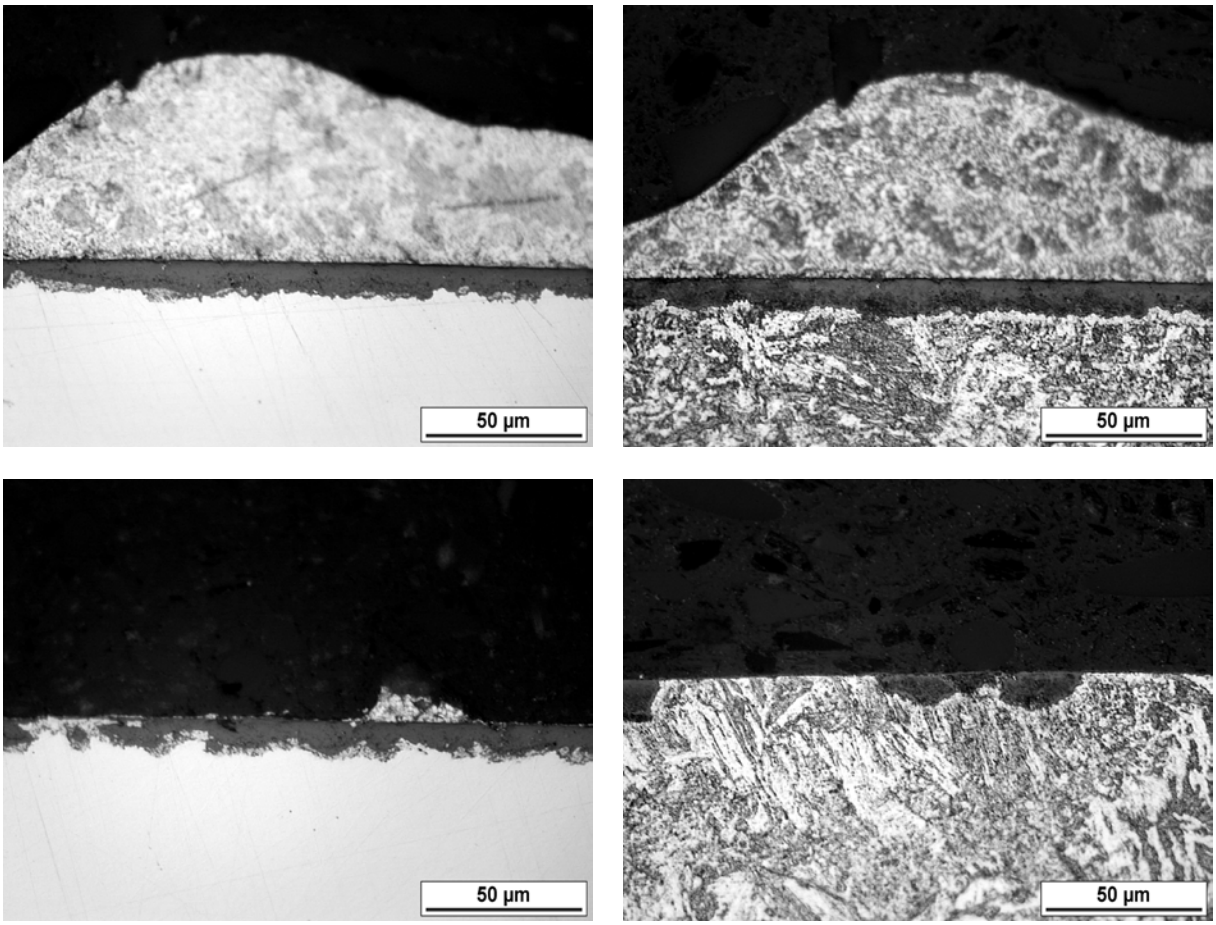

Figure 12 – *Oxide scales found in the vertical cross-section of the weld seam after exposure for 816 h in the CORRIDA loop at 550°C and $c_O \approx 5\times10^{-7}$ mass-%. Top row: Continuous spinel layer with local internal oxidation after polishing (left) and after etching with Röchling's solution (right). Bottom row: Non-uniform spinel layer with pronounced internal oxidation (left) and local spinel formation (right; after etching).*

tures which were introduced in the previous section, i.e., spinel formation occurring both locally and as a non-uniform continuous layer, accompanied by more or less pronounced internal oxidation. This means, that the presence of a thin (Cr-rich) scale and local spinel formation, along with a continuous spinel layer, is characteristic for the (short-term) oxidation behaviour of (materials similar to) P122 also at a stable higher oxygen concentration (remember that the results on short-term oxidation described in the previous section were obtained from exposures at varying oxygen concentrations).

After exposure for 2016 h, a non-uniform but mostly continuous spinel layer, accompanied by more or less pronounced internal oxidation, is characteristic for the oxidation behaviour of the weld seam in flowing LBE at 550°C and $c_O \approx 5\times10^{-7}$ mass-% (Figure 13). The nearly completed transition from local spinel formation to a continuous scale is an effect of the longer exposure time. Also after the exposure for 4990 h, the oxidation behaviour found for the weld seam qualitatively coincides with the behaviour of P122 after the standard heat-treatment. However, Cr-depleted peaks in the steel surface are more numerous and partial spalling of the spinel layer is more

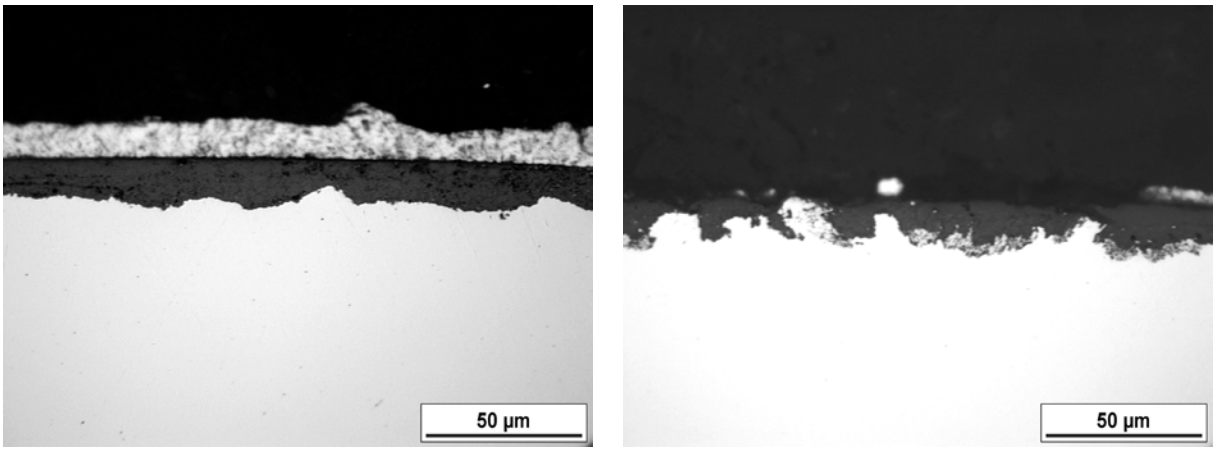

Figure 13 – *Oxide scales on the weld seam after exposure for 2016 h in the CORRIDA loop at 550°C and $c_O \approx 5\times10^{-7}$ mass-%.*

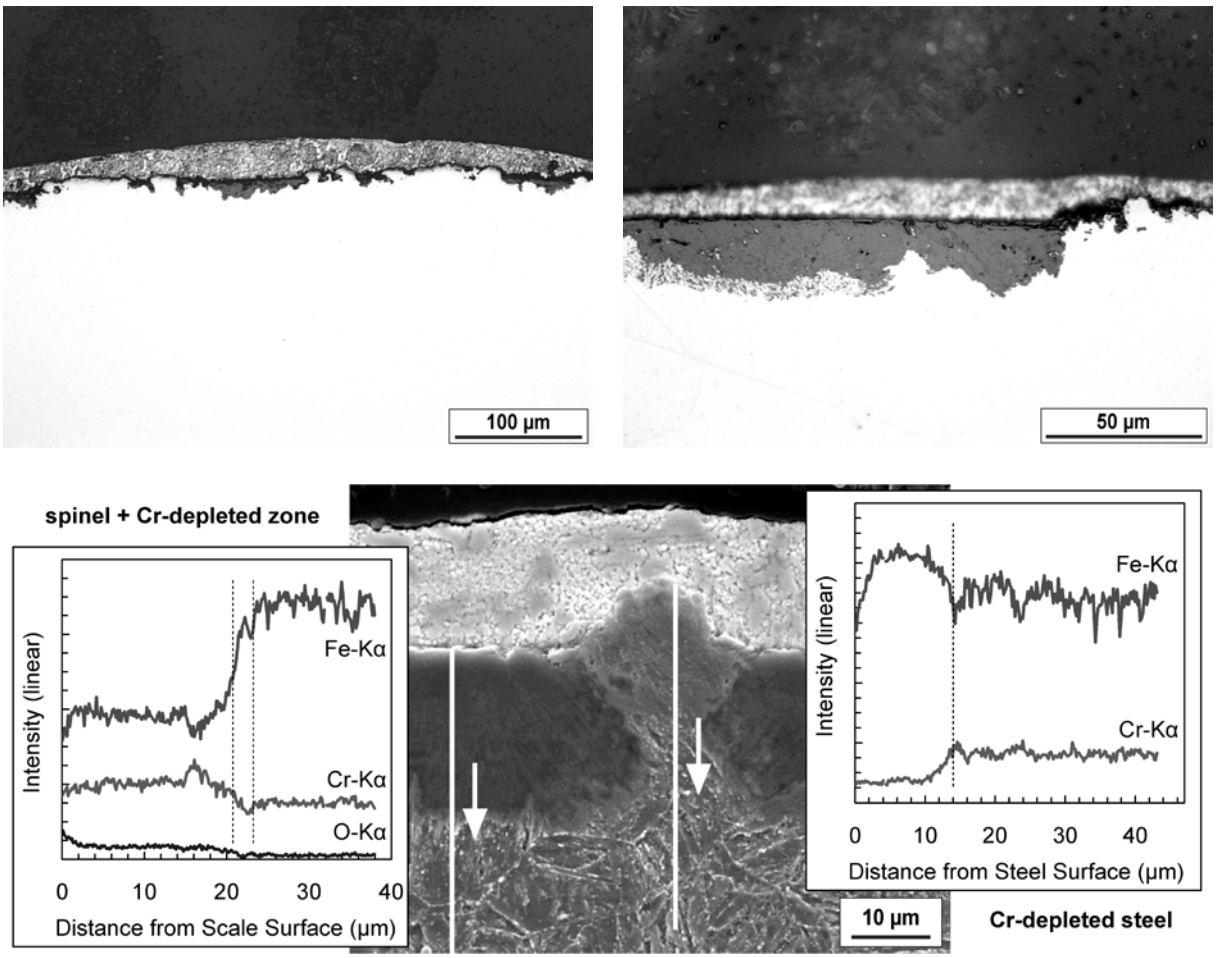

Figure 14 – *Vertical cross-section of the weld seam after exposure for 4990 h in the CORRIDA loop at 550°C and $c_O \approx 5\times10^{-7}$ mass-%. Top row: Partially spalled spinel layer and local internal oxidation. Bottom: Qualitative EDX-linescans along the adherent part of the spinel (left) and a Cr-depleted steel protrusion (right). Beneath the adherent spinel, the steel is also depleted in Cr.*

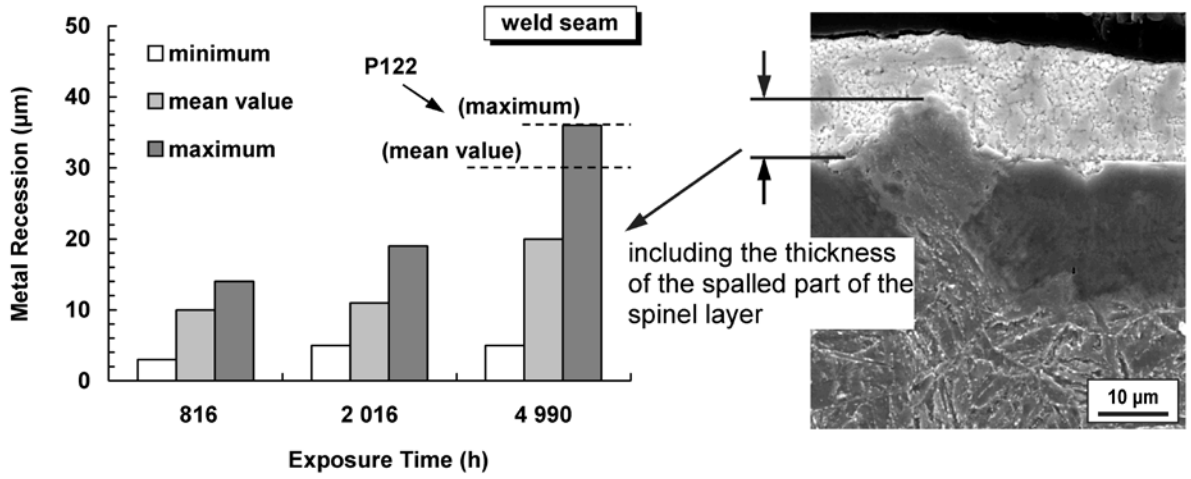

Figure 15 – *Metal recession (spinel layer + internal oxidation zone) of the weld seam after exposure to flowing LBE at 550°C and $c_O \approx 5\times10^{-7}$ mass-%. In the case of the exposure for 4990 h, the thickness of the spalled part of the spinel layer was estimated using the "free height" by which the Cr-depleted peaks in the steel surface exceed the surface of the adherent spinel.*

pronounced in the case of the weld seam (Figure 14). As will be shown in the following sub-section, the whole specimen from the welded plate (not only the weld seam) exhibits this slightly different oxidation behaviour which, accordingly, might result from the post-welding heat-treatment rather than properties which are specific to the weld seam.

The results of measurements of the metal recession – determined again from the thickness of the spinel layer and the internal oxidation zone – in the domain of the weld seam are summarised in Figure 15. In order to obtain a representative number of measurements along the specimen circumference (12), also sites where partial spalling of the spinel was evident had to be considered in the case of the exposure experiment for 4990 h; this was done by estimating the thickness of the spalled part of the spinel layer using the "free height" of the peaks in the steel surface (Figure 15). Although the real metal recession in the domain of the weld seam might be slightly underestimated by this method, Figure 15 shows that the oxidation behaviour of the weld seam is also quantitatively comparable to that of P122 (after the standard heat-treatment).

Up to this point, the behaviour of the weld seam in the course of a "regular" oxidation process in which the LBE participates only indirectly (as solvent for oxygen and steel constituents, e.g., Fe; probably also as erosive medium etc.) was described. Each specimen, however, shows one to two sites in the domain of the joint where an enhanced oxidation process took place, resulting in shallow pits in the material surface (Figures 16-18). In these cases, the LBE directly participated in the metal consumption (indicated by LBE which penetrated the steel beneath an oxide scale) and significant dissolution of steel constituents in the LBE is evident from the ratio of the local material loss to the amount of oxides adhering to the surface (especially after exposure for 2016 h; Figure 17). The structure (composition) of the oxide scale changes, exhibiting exceptionally Fe-rich and Cr-rich, respectively, oxides along with

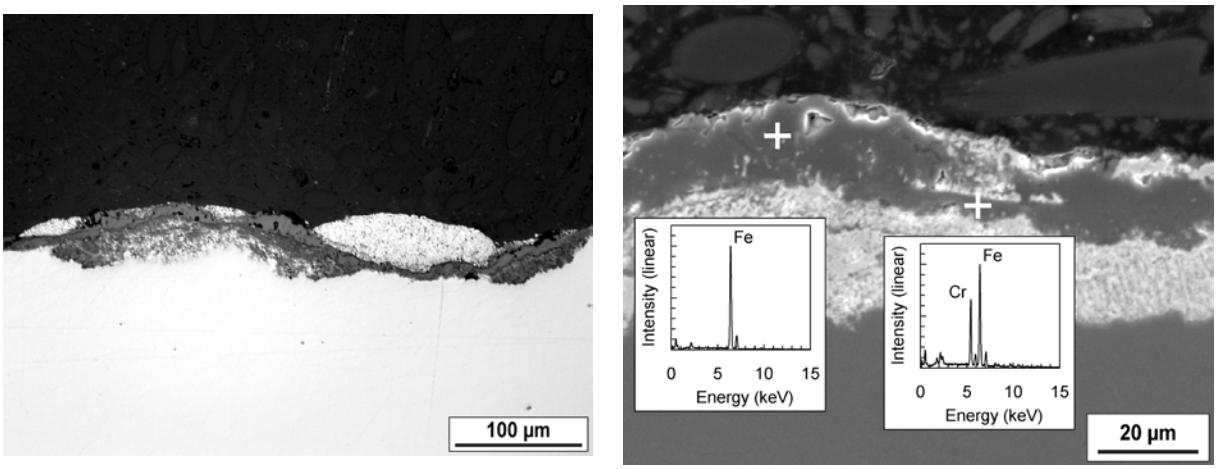

Figure 16 – *Liquid-metal assisted oxidation of the weld seam observed after exposure for 816 h (550°C; $c_O \approx 5\times10^{-7}$ mass-%). Left: Light-optical micrograph of affected site. Right: Electron-optical micrograph and results of qualitative EDX-analyses. The bright zone beneath the oxides contains Pb/Bi which penetrated the steel.*

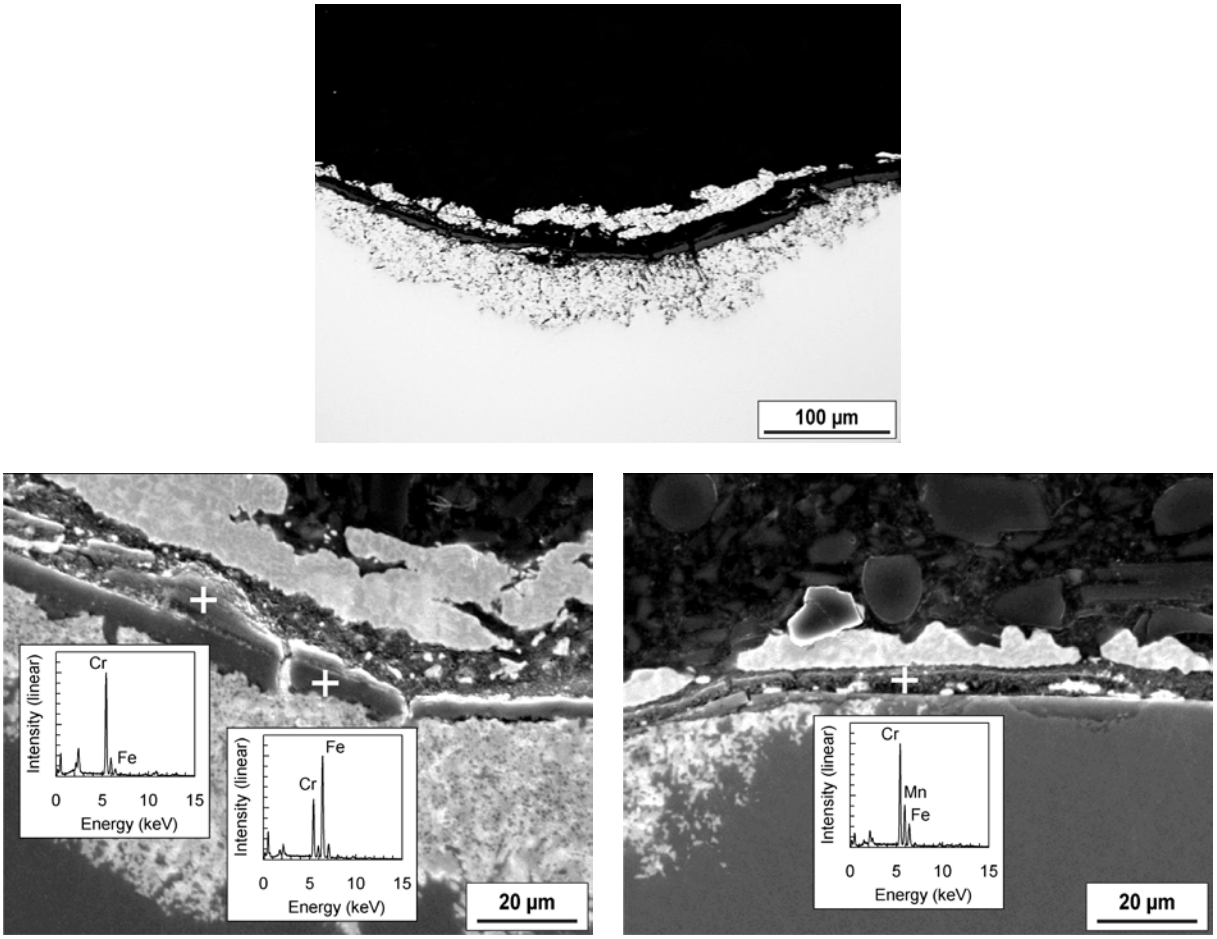

Figure 17 – *Liquid-metal assisted oxidation of the weld seam observed after exposure for 2016 h (550°C; $c_O \approx 5\times10^{-7}$ mass-%). Top: Light-optical micrograph of affected site. Bottom: Electron-optical micrographs and results of qualitative EDX-analyses. The bright zone beneath the oxides contains Pb/Bi which penetrated the steel.*

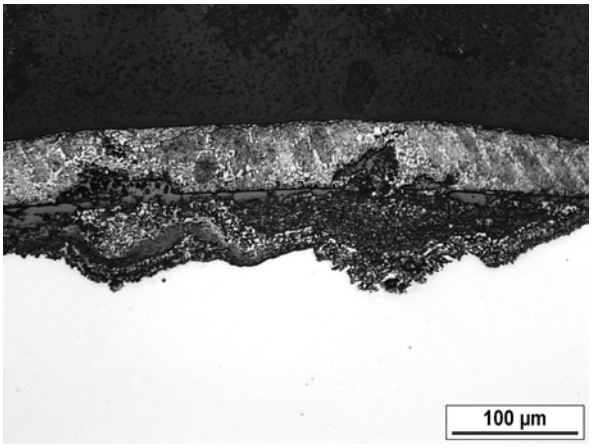

Figure 18 – *Liquid-metal assisted, enhanced oxidation of the weld seam observed after exposure for 4990 h (550°C; $c_O \approx 5\times10^{-7}$ mass-%).*

the (Fe,Cr) spinel which is characteristic for the scales formed in the course of regular oxidation; adjacent to one of the observed pits, a significant enrichment of Mn in the oxide scale became evident from qualitative EDX-analyses (Figure 17 bottom right). Imperfect overlapping of layers within the multi-run weld (*cf.* Figure 1) or compositional inhomogeneities might be involved in the initiation of this liquid-metal-assisted, enhanced corrosion, which can only be clarified with a detailed metallographic analysis of the joint. The local metal recession resulting from this type of corrosion – which depends on the time between the initiation of the underlying processes and the end of the exposure rather than the overall exposure time – is approximately 50, 120 and 78 µm after exposure for 816, 2016 and 4990 h, respectively.

Significant differences in the oxidation behaviour of the weld seam between the two test-sections of the CORRIDA loop were not observed, neither in the case of regular oxidation nor with respect to enhanced oxidation.

5.2 Transition zone and welded P122

Both the transition zone (Figure 19) and the welded steel (Figure 20) exhibit a behaviour similar to that of the weld seam. There are slight differences in the frequency of occurrence of the features which are specific for the exposure times – local spinel formation, continuous (non-uniform) spinel layers, internal oxidation, partial spalling of the spinel layer and Cr-depleted peaks in the steel surface – between the individual domains. These differences, however, are not clear enough to infer a general trend.

A quantitative comparison of the oxidation behaviour of the welded steel (P122 after the post-welding heat-treatment) and P122 after the standard heat-treatment is shown in Figure 21. The recession of the welded steel was estimated using the thickness of the spinel layer and the internal oxidation zone which were measured in the longitudinal cross-section of specimens after exposure. According to these measurements, there is no significant difference in the metal recession due to regular oxi-

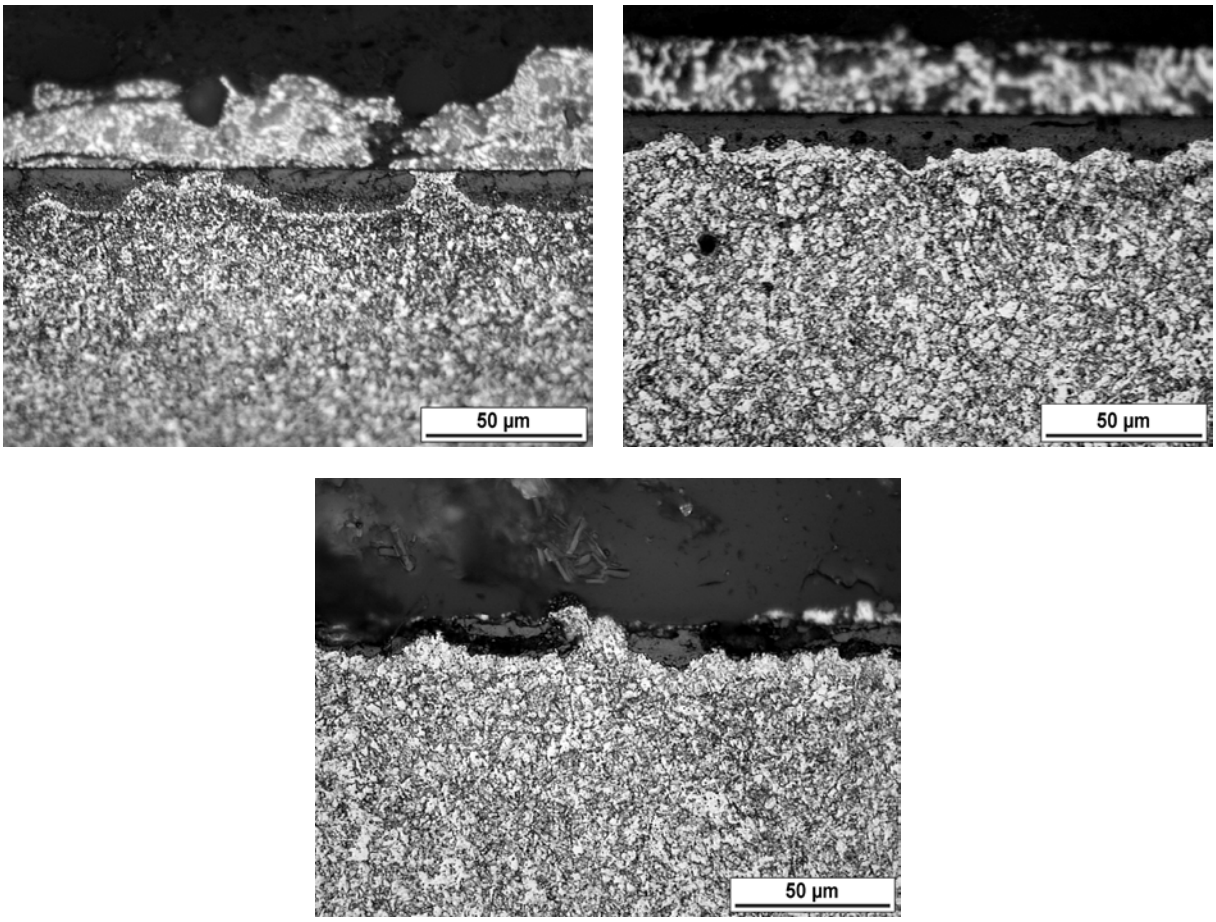

Figure 19 – *Oxide scales on the transition zone after exposure to flowing LBE at 550°C and $c_O \approx 5\times10^{-7}$ mass-%. Light-optical micrographs of longitudinal cross-sections after etching with Röchling's solution. Top left: discontinuous spinel scale after exposure for 816 h. Top right: continuous spinel layer after exposure for 2016 h. Bottom: partially spalled spinel layer and steel protrusions after exposure for 4990 h.*

dation between welded P122 and the steel after the standard heat-treatment. The same is true when welded P122 is compared with the weld seam.

In the course of the exposure for 816 h, both the transition zone and welded P122 were only affected by regular oxidation. The specimens exposed for 2016 and 4990 h, however, exhibited one site each where the LBE directly participated in the oxidation of welded P122 (Figure 22). Iron oxide is observed in the oxide scale formed in the course of this liquid-metal assisted, enhanced corrosion. Although the comparison of Figures 16, 17 and 22 implies that the structure of the corrosion scale and the effect of this type of corrosion can differ between the weld seam and welded P122, this different appearance of the attack probably results from the position of the specific section planes relative to the affected site (e.g., section through the centre of the affected site or close to the boundary). The major difference between regular and liquid-metal assisted oxidation seems to be that, in the latter case, the ingress of Pb and Bi into the steel enhances transport of Fe (and especially of Cr) via the liquid-metal phase and, therefore, consumption of the steel.

As in the case of the weld seam, the post-test examination did not deliver an unequivocal clue why liquid-metal assisted, enhanced corrosion starts in the case of welded P122 and not for P122 after the standard heat-treatment. The post-welding heat-treatment can play a role, but, considering the size of the specimens, the infrequent occurrence of this type of corrosion hints at a local peculiarity, e.g., an inhomogeneity in the welded plate. A laborious metallographic examination of the material might be necessary to clear this point.

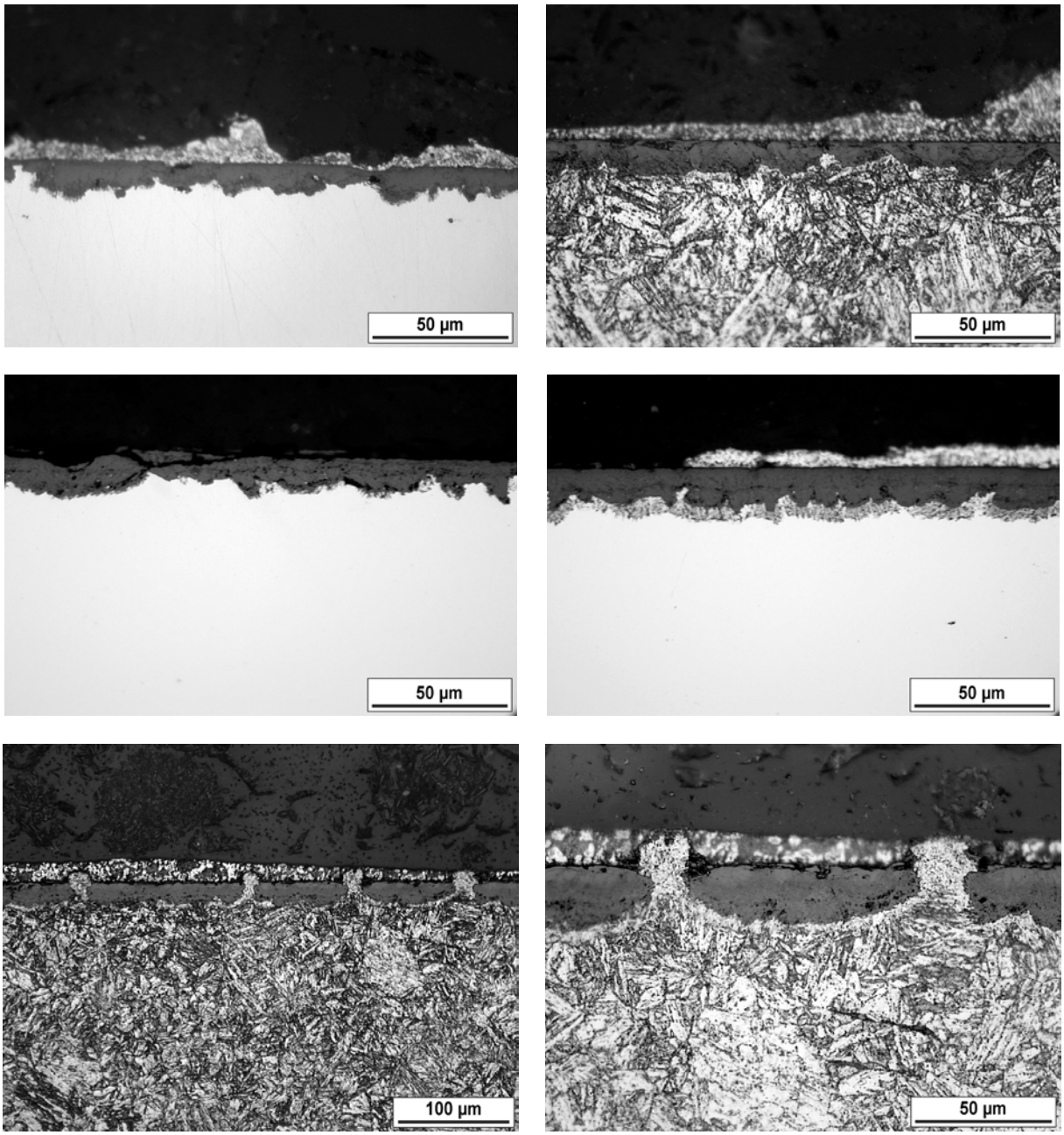

Figure 20 – *Oxide scales on the welded steel after exposure in the CORRIDA loop at 550°C and $c_O \approx 5\times10^{-7}$ mass-%. Light-optical micrographs of longitudinal cross-sections. Top row: non-uniform spinel layer after exposure for 816 h. Middle row: continuous spinel scales with more or less pronounced internal oxidation after exposure for 2016 h. Bottom row: partially spalled spinel layer and steel protrusions after exposure for 4990 h. Note the brighter appearance of the Cr-depleted peaks in the steel surface after etching with Röchling's solution.*

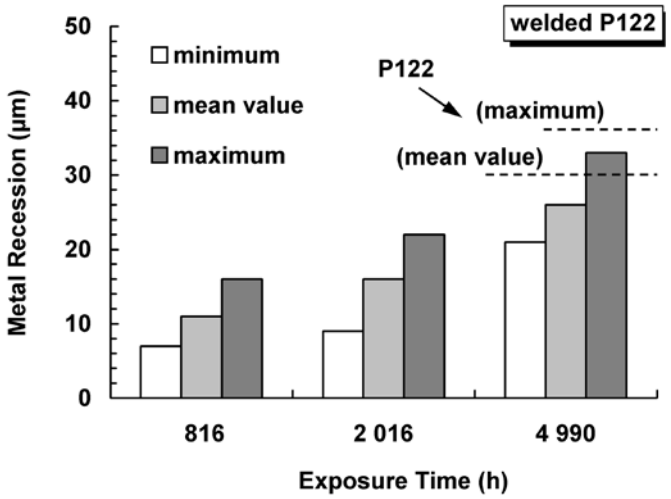

Figure 21 – *Metal recession due to regular oxidation of the welded steel (P122 after the post-welding heat-treatment) after exposure to flowing LBE at 550°C and $c_O \approx 5\times10^{-7}$ mass-%. For 7 of the 12 individual measurements after exposure for 4990 h, the thickness of the spalled part of the spinel layer was added using the free height of adjacent peaks in the steel surface (cf. Figure 15).*

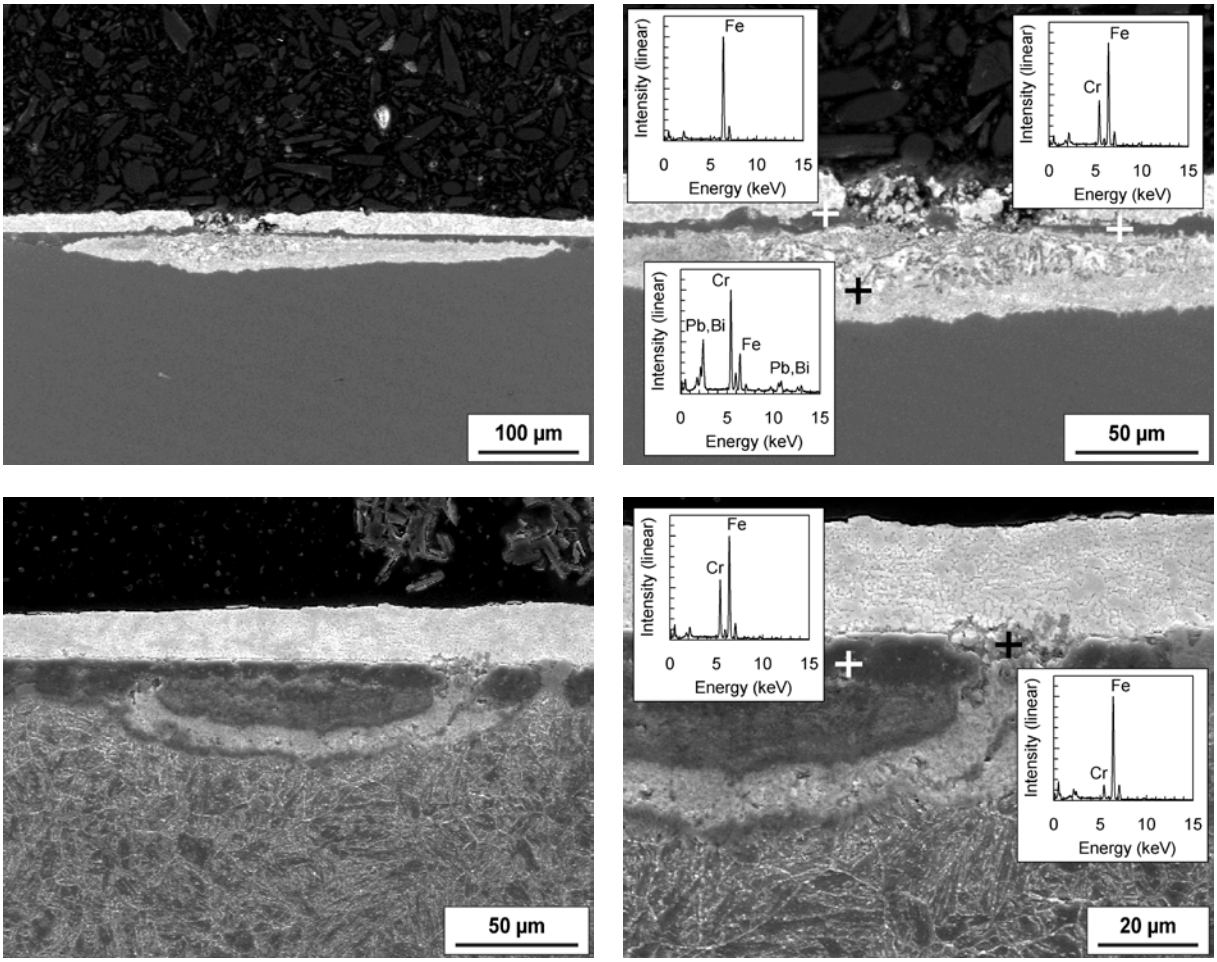

Figure 22 – *Liquid-metal assisted, enhanced corrosion of welded P122 observed after exposure for 2016 (top) and 4990 h (bottom) at 550°C and $c_O \approx 5\times10^{-7}$ mass-%. Electron-optical micrographs of affected sites after etching with Röchling's solution and results of qualitative EDX-analyses. The bright zone beneath the oxides contains Pb/Bi which penetrated the steel.*

Significant differences in the (qualitative) oxidation behaviour of the transition zone and welded P122 between the two test-sections of the CORRIDA loop were not observed.

5.3 Influence of surface-alloying with aluminium (GESA-treatment)

Figure 23 shows light-optical micrographs of the aluminised surface layer on the weld seam (longitudinal cross-section) after exposure to flowing LBE at 550°C and $c_O \approx 5\times10^{-7}$ mass-% for 4990 h. No significant oxidation and no liquid metal corrosion was observed within this domain. Apparently, a thin protective Al-rich oxide scale formed on the surface which prevents any further remarkable reaction of oxygen or LBE with the constituents of the material. Also, no significant corrosion was observed in the transition zone after surface-alloying with aluminium (Figure 24).

Only in the domain which accounts for welded P122, some defects (vertical cracks) within the aluminised surface layer resulted in local corrosion along these defects and of the steel beneath the surface layer (Figure 25). The reason for this is most likely not specific to the welded steel, but follows from the vicinity of this domain to the specimen edges where the quality of the aluminised surface layer is not as high as in the centre of the specimen.

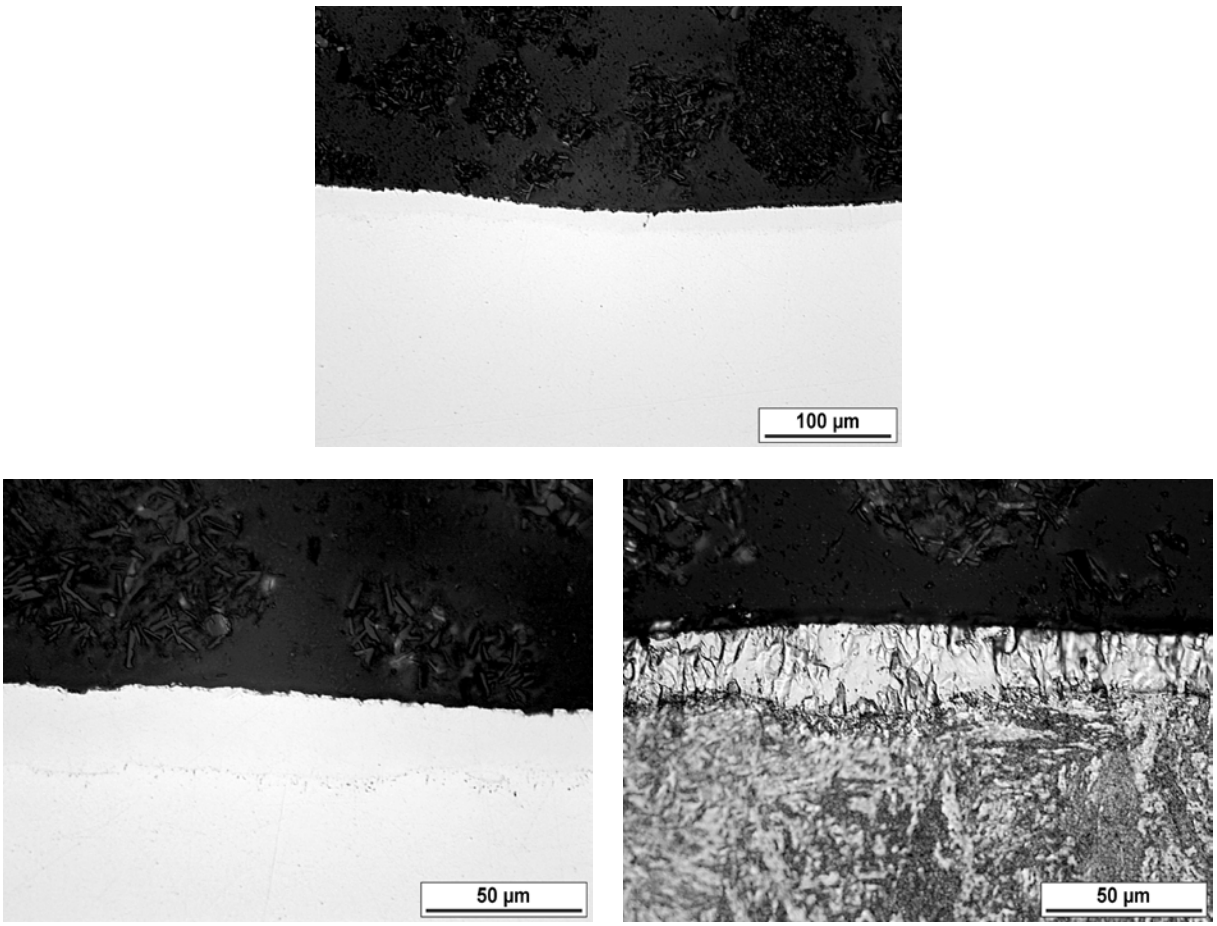

Figure 23 – *Longitudinal cross-section of the aluminised surface layer on the weld seam after exposure to flowing LBE at 550°C and $c_O \approx 5\times10^{-7}$ mass-% for 4990 h. Bottom right: after etching with Röchling's solution.*

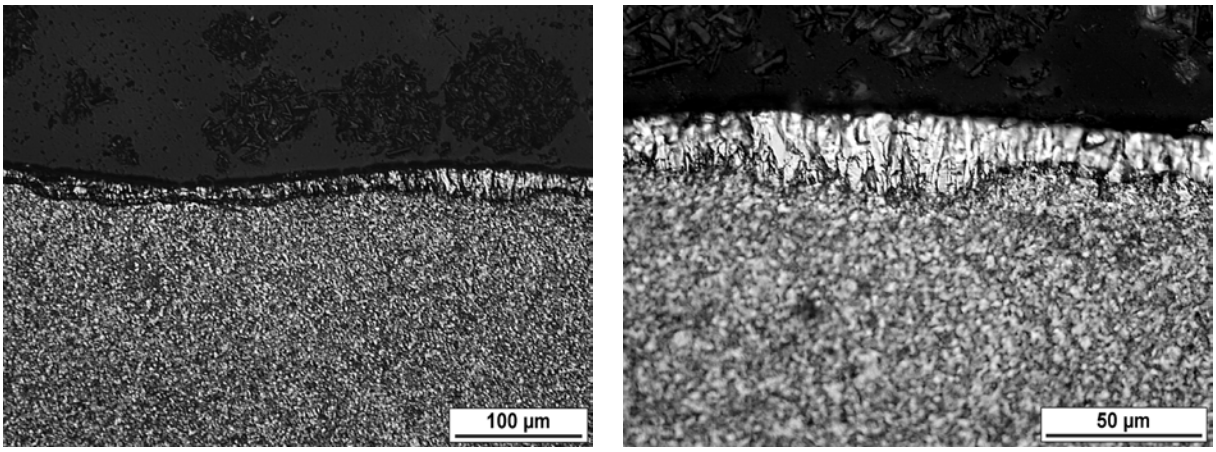

Figure 24 – *Aluminised surface layer on the transition zone after exposure to flowing LBE at 550°C and $c_O \approx 5\times10^{-7}$ mass-% for 4990 h. Longitudinal cross-section after etching with Röchling's solution.*

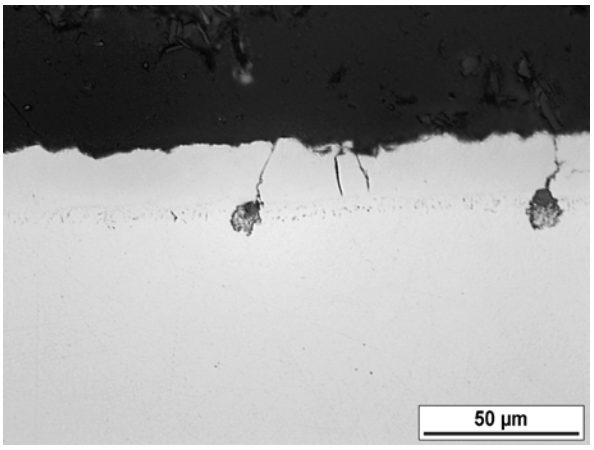

Figure 25 – *Defects within the aluminised surface layer on welded P122 (in thevicinity of the specimen edges!) after exposure to flowing LBE at 550°C and $c_O \approx 5\times10^{-7}$ mass-% for 4990 h.*

6 Conclusions

- The behaviour of the three domains of P122 joined by multi-layer TIG welding – the weld seam, a transition zone and the welded steel (P122 after the post-welding heat-treatment) – in flowing LBE at 550°C and $c_O \approx 5\times10^{-7}$ mass-% is, generally comparable to that of P122 after the standard heat-treatment, both qualitatively and quantitatively. The estimated maximum metal recession (material consumption) of the weld seam in the course of "regular" oxidation is 36 µm after 4990 h (0.06 mm/y).

- Few exceptions from the regular oxidation behaviour occurred in the case of the weld seam and the welded steel. In these cases, the LBE directly participated in the corrosion processes resulting in a locally enhanced metal recession. The infrequent occurrence implies local peculiarities of the specific sample material (e.g., compositional inhomogeneities, imperfect overlapping of layers within the weld)

as the most probable reason for the onset of this type of corrosion. A more detailed (metallographic) analysis of the sample material may clear this point.

- The exposure of GESA-treated specimens showed that surface-alloying with aluminium prevents significant oxidation and liquid metal corrosion also in the case of P122 joined by welding.

References

[1] G. Müller, A. Heinzel, G. Schumacher, A. Weisenburger, J. Nucl. Mater. 321 [2-3] (2003) 256-262.
[2] G. Müller, G. Schumacher, F. Zimmermann, J. Nucl. Mater. 278 [1] (2000) 85-95.